

Cite this: *RSC Sustainability*, 2023, 1, 2350

# Recovery of palladium from waste fashion items through food waste by-products†

Teresa Cecchi,<sup>†</sup> Zhaojing Gao,<sup>†</sup> Christophe Clement,<sup>b</sup> Yasser Matos Peralta,<sup>b</sup> Olivier Girard<sup>b</sup> and Clara Santato<sup>†</sup>

Palladium is a non-toxic platinum group metal indispensable for several industrial applications. It is among the 44 endangered elements; hence, its recycling from secondary sources is crucial. Waste plated metal wires from the fashion industry are an important waste stream for this precious metal. We propose a sustainable route for Pd recovery where palladium peels off in its metallic state in a single-step, room-temperature process. At the same time, readily oxidizable base metals are leached under very mild conditions using a green oxidant, hydrogen peroxide, and lactic acid, a food chain byproduct. This strategy is chemically rational, cost-effective, and environmentally friendly. The recovered Pd was successfully recycled to fabricate source and drain electrodes in organic field-effect transistors. Waste wires, recovered palladium flakes, and e-beam evaporated Pd electrodes were characterized by scanning electron microscopy, energy dispersive spectroscopy, X-ray photoelectron spectroscopy, and atomic force microscopy to examine their morphology and (surface) chemical composition.

Received 14th July 2023  
Accepted 15th October 2023

DOI: 10.1039/d3su00242j

rsc.li/rscsus

## Sustainability spotlight

This manuscript reports on sustainable Pd recovery from waste fashion items by a chemical route where palladium peels off in its metallic state, while readily oxidizable base metals are leached under very mild conditions using a mild oxidant, hydrogen peroxide, and lactic acid, a food chain byproduct. It contributes to developing a circular vision in the broad range of industries using metals, e.g., aerospace, electronics, automotive and fashion. The route we propose is safe and affordable. Its design is rational, since the route avoids the reduction step from the cationic to the metallic form that is required by routes already available in the literature. Our research contributes to the achievement of the UN SDG, e.g., 11 (Sustainable Cities and Communities) and 12 (Responsible Consumption and Production).

## Introduction

Pd is mainly used in catalysis, particularly in automotive catalytic converters.<sup>1–4</sup> The increasing demand for car engines continues to deplete platinum group metal ores,<sup>5–7</sup> placing Pd among endangered elements.<sup>8,9</sup> Finely divided Pd serves as a catalyst in hydrogenation and dehydrogenation reactions, while heated Pd facilitates hydrogen purification through diffusion.<sup>10</sup> Pd-based galvanic coatings for jewellery and fashion items are another important industrial use of this precious metal.

Pd is commercially obtained as a by-product of nickel, copper and zinc refining,<sup>11</sup> through an energy-intensive, high environmental impact refining process,<sup>12,13</sup> such that the

selective recovery of Pd from secondary sources becomes crucial. There are waste streams that can provide a closed-loop and sustainable source of Pd, such as spent catalytic converters (SCCs) and electronic waste (e-waste). Here, the concentration of Pd (2000 g per tonne in SCCs and 300 g per tonne in e-waste) is higher than in natural ores (<10 g per tonne), such that urban mining of these important secondary sources is environmentally and economically viable.

Among others, pyrometallurgical or hydrometallurgical processes are available for Pd recovery.<sup>14–17</sup>

The pyrometallurgical route is energy-intensive with high environmental impact, given the high melting point of Pd (1550 °C). Hydrometallurgy makes use of an oxidant and a lixiviant (usually aqua regia and cyanide) to dissolve metals. The resulting leaching solution contains several metal ions. Unfortunately, the strategies for Pd isolation are expensive and labor-intensive.<sup>16</sup> Hence, different physiochemical routes have been explored to recover Pd from multi-metal leaching solutions: solvent extraction,<sup>3,18,19</sup> strong basic anionic resin,<sup>20</sup> molecular recognition,<sup>21</sup> solid sorbents<sup>3,22–25</sup> and Pd(II) photodeposition.

<sup>a</sup>Istituto Tecnico Tecnologico (ITT) G. and M. Montani, 63900, Fermo, Italy. E-mail: cecchi.teresa@istitutomontani.edu.it

<sup>b</sup>Engineering Physics, Polytechnique Montreal, H3T 1J4, Montreal, QC, Canada. E-mail: clara.santato@polymtl.ca

† Electronic supplementary information (ESI) available. See DOI: <https://doi.org/10.1039/d3su00242j>

‡ These authors equally contributed.



In bio-hydrometallurgical routes, microorganisms are used to leach Pd, *e.g.*, using bacterial cyanogenesis for the *in situ* production of cyanide.<sup>17</sup> Microorganisms can also separate Pd(II) by bio-reduction, bio-precipitation, chelation, extracellular sequestration, biosorption and metal uptake.<sup>26</sup> Plants' metabolites, including phenols, saponins, alkaloids, organic acids, proteins, *etc.*, can reduce metal ions.<sup>16</sup>

Considering the state-of-the-art we just presented, we thought about designing and demonstrating the proof of principle of a more sustainable process for Pd recovery based on the leaching under mild conditions (enabled by their high oxidizability) of base metals present together with Pd in the Pd-including waste while peeling off Pd in its metallic state.<sup>27</sup> In this way, the precious metal is recovered while avoiding the reduction step transforming its cationic form to the metallic one, that is the illogical core strategy shared by all other procedures.

In this work, we report on Pd peeling from waste metal wires from the galvanic fashion industry by using a mild oxidizing agent, H<sub>2</sub>O<sub>2</sub>, in an acidic environment obtained by using lactic acid, a by-product of the food industry. The Pd-coated waste wires were used to hold fashion items during their plating and underwent the same plating process as the fashion items themselves. After removal from the wires' surface, Pd was obtained in the metallic form, without any need for reduction. The peeled Pd flakes were characterized by scanning electron microscopy (SEM), energy dispersive spectroscopy (EDS), X-ray photoelectron spectroscopy (XPS), and atomic force microscopy (AFM) for their morphology and (surface) chemical composition and bonding. Furthermore, we successfully used the flakes to e-beam evaporate source and drain electrodes in organic field-effect transistors. Our approach to Pd recovery paves the way to safe, sustainable and economically affordable Pd recovery and recycling.

## Experimental

### Waste metal wires

Waste Pd-plated metal wires were a gift from GPS Galvanica (Montegiorgio, FM, Italy) and Settimi Galvanica (Macerata, Italy). Those copper-based wires are used to hold fashion items to be plated, such that they undergo the same process as the fashion items. The plating process is described in the ESI.† Waste Pd-plated metal wires were used as received, without any mechanical treatment.

### Reagents

L-Lactic acid (2-hydroxy-propionic acid, 80% w/w, food, and cosmetic grade, obtained from vegetable carbohydrate fermentation, 1.19 g ml<sup>-1</sup>, 10.6 M; heavy metals <10 ppm, mercury and arsenic <1 ppm, lead <0.5 ppm, and calcium and sulfates <20 ppm) was obtained from Farmalabor (Canosa di Puglia, BAT, Italy). Hydrogen peroxide 35% w/w (1.130 g ml<sup>-1</sup>, 11.6 M) was obtained from Italcimici Group. Ultrapure water was produced *via* a Millipore Simplicity® UV system.

Commercial palladium was purchased from Kurt J. Lesker company with a purity of 99.95%.

### Palladium peeling

Systematic experiments were carried out to optimize peeling efficiency, reagents' concentrations, reaction time, and temperature to avoid the Fenton reaction.

The optimal reaction mixture was obtained by adding 8 L of a solution of lactic acid and hydrogen peroxide, respectively 2.11 M and 2.33 M in ultrapure water (1.6 L of lactic acid 80% w/w, 1.6 L of hydrogen peroxide 35% w/w and 4.8 L of ultrapure water) to 320 g of waste metal wires in a reaction vessel (made of High-Density Poly Propylene (HDPP)), under a fume hood. The final solution : waste metal wire ratio was 25 ml g<sup>-1</sup>. The mixture was left at room temperature. Pd peeling was visually monitored. After 6 h, the base metals' leaching was complete, and the wires were washed and removed. Thin and tiny Pd flakes stripped from the metal wires were separated from the solution of base metal ions *via* vacuum filtration, using a Gooch crucible, and washed with 50 ml ultrapure water 6 times. They were dried overnight at 180 °C and weighed to calculate the yield of recovery.

### Scanning electron microscopy (SEM) and energy dispersive spectroscopy (EDS)

SEM was employed to examine wires, flakes, and e-beam evaporated electrodes obtained from the flakes (*vide infra*). The experiments were conducted at an accelerating voltage of 5 kV, utilizing both backscattered electron and secondary electron imaging modes, with a JEOL FEG-SEM. We also analyzed the chemical composition of the samples through an X-Max + Energy Dispersive Spectrometer (EDS) from Oxford Instruments equipped with an 80 mm<sup>2</sup> active area SDD.

### X-ray photoelectron spectroscopy (XPS)

XPS analysis was carried out under vacuum (<10<sup>-8</sup> Torr) using Escalab 250Xi equipment (Thermo Fisher Scientific), equipped with a monochromated Al K<sub>α</sub> source at a power of 218.8 W (14.7 kV, 14.9 mA). The XPS full survey spectrum was acquired from 0 to 1350 eV, with a step size of 1 eV, dwell time of 100 ms and

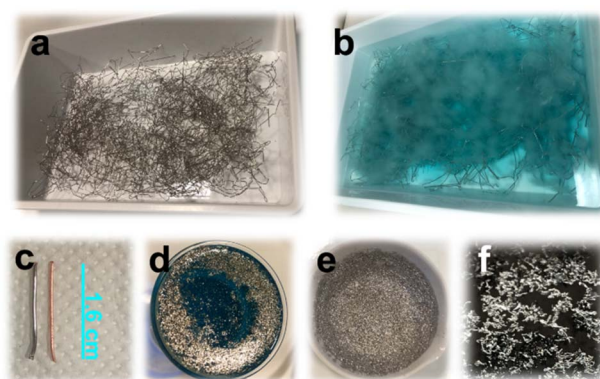
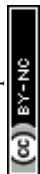


Fig. 1 Pd peeling from waste wires. (a) Pd plated waste wire in the open reaction vessel. (b) Reaction environment after 30 m at room temperature. (c) Pristine and peeled wires after a 6 h-long process. (d) Gooch vacuum filtration. (e) Dried and recovered Pd. (f) Pd peeled flakes.





Fig. 2 SEM images and corresponding EDS spectra of (a and b) waste wires; (c and d) peeled flakes from waste wires; (e and f) e-beam evaporated electrodes from recycled Pd; (g and h) e-beam evaporated electrodes from commercial Pd.



pass energy of 150 eV. Binding energies were referenced to the C 1s peak at 285.0 eV for aliphatic hydrocarbons.

### Atomic force microscopy (AFM) and contact angle

The surface morphology of electrodes and PCBM films was investigated by AFM. All images were taken in air at room temperature on a Digital Instruments Dimension 3100, in tapping mode, with Al-coated silicon cantilevers.

The contact angle was measured by using a contact angle surface tensiometer.

### Microfabrication of electrodes

Photolithography for metal electrode patterning was carried out on  $200 \pm 10$  nm-thick  $\text{SiO}_2$  on a  $525 \pm 25$   $\mu\text{m}$ -thick silicon wafer purchased from WaferPro, San Jose, California. Interdigitated circular Pd/Ti electrodes ( $40$  nm/ $5$  nm) had a width ( $W$ ) of  $2.5$   $\mu\text{m}$  and an interelectrode distance ( $L$ ) of  $10$   $\mu\text{m}$ . The thickness of the evaporated recycled Pd electrodes was  $59 \pm 1$  nm, whereas that of the electrodes deposited from commercial Pd was  $48 \pm 1$  nm. For e-beam evaporation, Pd peeled flakes were compressed into pellets using a laboratory Pellet Press PP25. The patterned substrates were cleaned with a sequential ultrasonic bath in isopropanol alcohol (IPA), acetone, and IPA, followed by UV ozone exposure prior to the deposition of the semiconducting thin films.

### Semiconducting film fabrication and transistor characterization

Thin films of phenyl-C61-butyric acid methyl ester (PCBM, Solaris Chem) were spin-coated ( $1500$  rpm,  $100$  s) on source and drain pre-patterned  $\text{SiO}_2/\text{Si}$  substrates from a  $10$  mg  $\text{ml}^{-1}$  solution in chlorobenzene, under a  $\text{N}_2$  atmosphere ( $\text{O}_2 < 3$  ppm and  $\text{H}_2\text{O} < 3$  ppm). Prior to spin-coating, the solution was stirred overnight. After spin coating, all devices were thermally treated on a hotplate at  $50$   $^\circ\text{C}$  for  $2$  h. Transistor characterization was performed by using a semiconductor parameter analyzer, Agilent B1500A, on a home-made electrical probe station inside a  $\text{N}_2$  glove box, at room temperature.

## Results and discussion

### Sustainable approach to Pd peeling

A sustainable approach to peel Pd from waste metal wires is based on a good oxidant that oxidizes the base metals without oxidizing Pd in an acidic reaction environment. Hydrogen peroxide is widely used in hydrometallurgical processes because it is a safe, effective, powerful (standard potential  $1.78$  V *versus* the standard hydrogen electrode), and versatile oxidant.<sup>28</sup> Base metals, *e.g.*, copper and nickel, reduce hydrogen peroxide according to the following reaction:



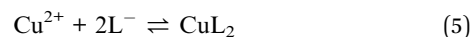
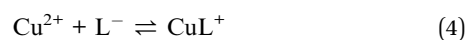
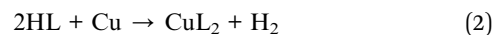
The non-toxicity of the reduction product (water) is noteworthy. In our case, for the acidic environment, we used lactic acid, a biobased platform chemical<sup>29</sup> obtainable from the



Fig. 3 XPS full survey spectra of waste metal wires (a), peeled flakes (b), e-beam evaporated electrodes from recycled Pd (c) and commercial Pd (d) on  $\text{SiO}_2$ .

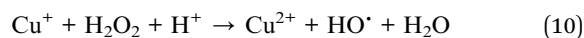
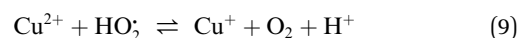
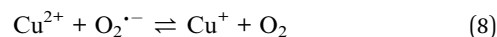
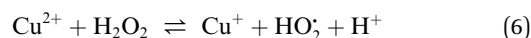
upcycling of a wide range of carbohydrate-containing food waste *via* bacterial fermentation.<sup>30</sup>

Lactic acid is known to dissolve copper<sup>31,32</sup> but also to complex metal ions, thereby providing an extra driving force for base metal leaching. If HL indicates lactic acid in the acidic pH range, copper can be solubilized as  $\text{Cu}^{2+}$ ,  $\text{CuL}^+$ , and, especially,  $\text{CuL}_2$  according to the following reactions:



The acidic dissociation of lactic acid is characterized by  $\text{pK}_a = 3.81$ . The stability constants for reactions (4) and (5) are  $2.45$  and  $4.08$ .<sup>33</sup>

The presence of copper ions in an acidic environment can trigger a Fenton-like reaction at room temperature and atmospheric pressure.  $\text{Cu}^{2+}$ -catalyzed Fenton-like processes can be described as follows:<sup>34,35</sup>



The hydroxyl radical is the main oxidant under acidic conditions. It is expected to further contribute to base metal



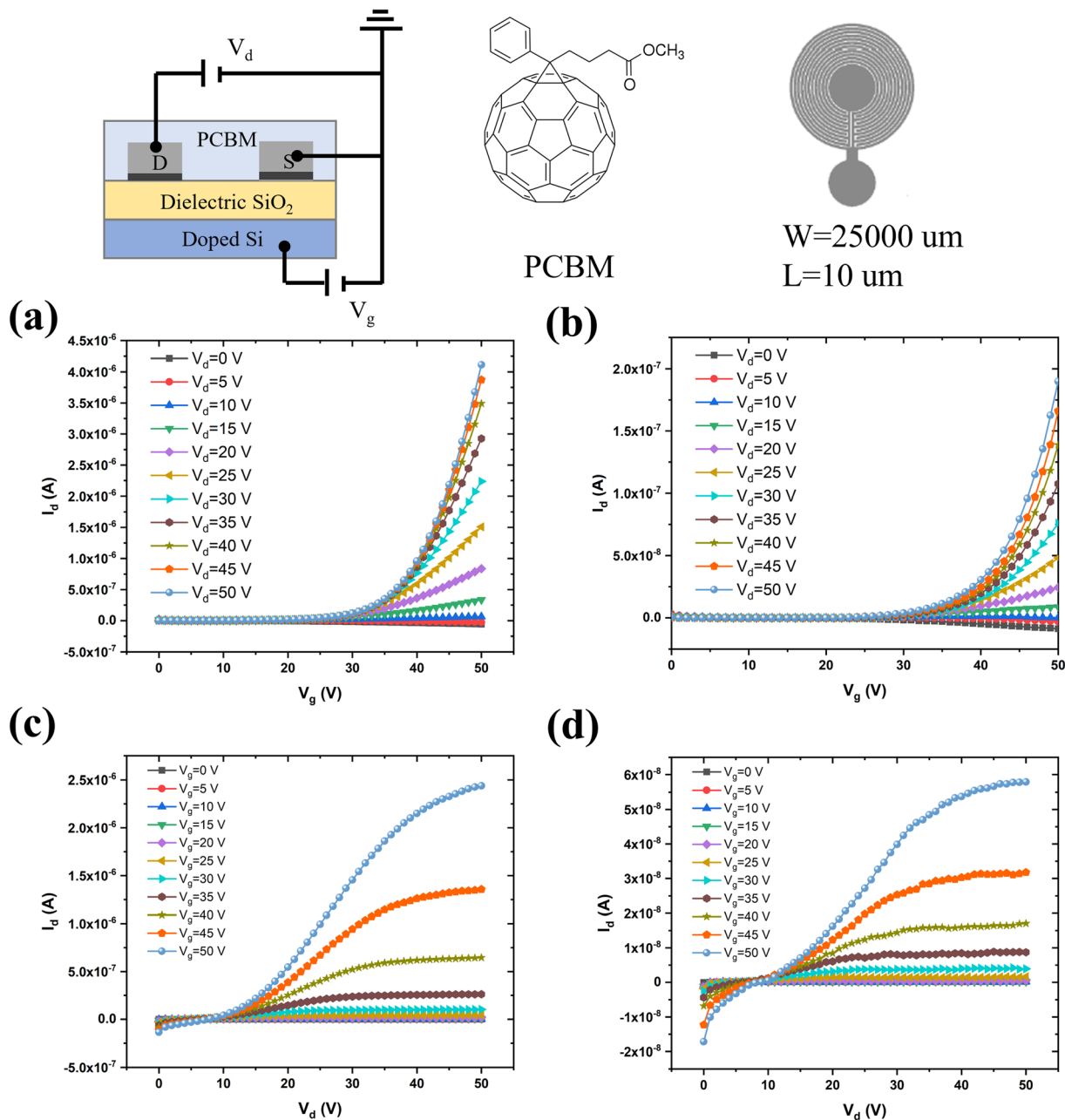


Fig. 4 Transfer (a and b) and output (c and d) characteristics of PCBM FETs based on Pd source and drain electrodes from recycled Pd (a and c) and commercial Pd (b and d). Top of the figure: scheme of PCBM FETs, the molecular structure of PCBM and electrodes' configuration.

oxidation due to its strong oxidation capacity (standard potential 2.80 V *versus* the standard hydrogen electrode).<sup>36</sup> Nickel(II) has been reported to enable the Fenton reaction, too.<sup>34</sup>

Preliminary experiments indicated that the energy-intensive heating of the mixture to achieve Pd peeling in a short time (1 h) is not safe. Indeed, the decomposition of H<sub>2</sub>O<sub>2</sub> by base metal ions is challenging to manage because base metal oxidation catalyzes the Fenton chemistry according to reactions in eqn (6)–(10). In turn, this produces the strongly oxidizing hydroxyl radical. Furthermore, the oxygen evolution is vigorous, and the process's exothermicity further accelerates the reaction.<sup>37</sup>

Hence, the initial heating of the mixture to shorten reaction times to 1 h is not recommended in the scale-up of the process for both safety and sustainability reasons.

Concerning the reactants' amounts, we progressively reduced the reagent concentrations to those indicated in the Experimental section (lactic acid and hydrogen peroxide, respectively, 2.11 M and 2.33 M) to obtain a safe and complete peeling of Pd in 6 h at room temperature. 0.6155 g of Pd were recovered from 320 g of raw metal wires with a yield of 0.19%. Fig. 1 includes the optical images of the Pd peeling process. When lactic and hydrogen peroxide concentrations were halved



to find the lowest amounts of reagents needed for a complete peeling, the reaction time increased to 24 h.

The solution volume to waste metal wire weight ratio is another important parameter; to avoid the Fenton reaction, such a ratio must be at least 25 ml g<sup>-1</sup>.

### SEM and EDS

Waste wires, peeled flakes, and e-beam evaporated electrodes from recycled and commercial Pd were studied by SEM and EDS (Fig. 2, S3 and Table S1†). The EDS spectra of the wire cross-section indicate the presence of Pd, Cu, Au, Ni, N, Zn, and O (Fig. 2b). EDS spectra from Pd flakes show mainly the presence of Pd (Fig. 2d), whereas those of the e-beam evaporated electrodes from recycled and commercial Pd show mainly Si, O, Ni, and Pd (Fig. 2f) and Si, Pd, O, and N (Fig. 2h).

### X-ray photoelectron spectroscopy (XPS)

The surface chemical composition of the wires, flakes, and e-beam evaporated electrodes from recycled and commercial Pd were investigated by XPS. The full survey spectra are presented in Fig. 3. Table S2† shows the atomic percentages and binding energies obtained from the XPS analyses performed on waste wires, peeled flakes, and e-beam evaporated electrodes from commercial and recycled Pd.

The main chemical species detected on the wires are Pd, C, and Cu. The detection of C is likely due to protective polymer coatings on the surface of the wires. The high-resolution scan, Fig. S2,† shows metallic Pd, Cu and their oxidized compounds. In the flakes, the elements Cu, Ni, Ag, Pd, C, and Cl were detected. The high-resolution scan, Fig. S3,† shows metallic Pd without oxidized compounds.

In e-beam evaporated electrodes from recycled Pd, survey scans showed the presence of Ni. High-resolution scans (Fig. S4†) showed that Ni is present as a mixture of metallic Ni and NiO.

Palladium is found only as a metal. In e-beam evaporated electrodes from commercial Pd, survey scans showed that Pd is the only metal (S was detected in these last samples too; high-resolution scans in Fig. S5† showed the S<sub>2p<sub>3/2</sub></sub> peak located at ca. 162 eV, which corresponds to S bonding to palladium).<sup>38</sup>

Elements detected by EDS and XPS are included in Table S1.†

### Transistor characterization

After the morphological and chemical characterization of the peeled flakes, we fabricated field-effect transistors based on e-beam evaporated source and drain electrodes, both from commercial and recycled Pd. We used the n-type organic semiconductor phenyl-C61-butyric acid methyl ester (PCBM, a soluble fullerene derivative) for the transistor channel material.<sup>39–42</sup> The output (drain-source current,  $I_{ds}$ , vs. drain-source voltage,  $V_{ds}$ , for increasing values of the gate-source voltage,  $V_{gs}$ ) and transfer ( $I_{ds}$  vs.  $V_{gs}$ , for increasing values of  $V_{ds}$ ) characteristics of the PCBM transistors were measured (Fig. 4). The mobility for transistors making use of commercial Pd, as deduced from the transfer characteristics at saturation, was 10<sup>-5</sup> cm<sup>2</sup> V<sup>-1</sup> s<sup>-1</sup> whereas it was 4.0 × 10<sup>-4</sup> cm<sup>2</sup> V<sup>-1</sup> s<sup>-1</sup> for transistors using recycled Pd. The threshold voltage was about 27 V for both types of transistors, and the ON/OFF ratio ( $I_{ON}/I_{OFF}$  calculated from  $I_{ds}$  measured between  $V_{gs} = 50$  V and  $V_{gs} = 0$  V, at  $V_{ds} = 50$  V) was ca. 10<sup>3</sup> and 3 × 10<sup>3</sup> for PCBM FETs based on commercial and recycled Pd, respectively.

The better performance of devices based on electrodes from recycled Pd than those based on commercial Pd could be due to several factors. One factor could be that the Ni–Pd alloy has a lower density (10–11.5 g cm<sup>-3</sup>) than pure Pd (12 g cm<sup>-3</sup>),<sup>43</sup> leading to electrodes thicker than those grown from commercial Pd under the same evaporation conditions. Another factor would be that the Ni–Pd alloy work function is lower (ca. 5.04–5.35 eV) than that of pure Pd (ca. 5.22–5.60 eV).<sup>44</sup> This would



Fig. 5 Atomic force microscopy (AFM) images of (a and e) the recycled Pd electrode surface; (b and f) commercial Pd electrode surface; PCBM thin films on Pd e-beam evaporated electrodes from (c and g) recycled Pd, (d and h) commercial Pd. 5 μm × 5 μm-sized images (a–d), and 2 μm × 2 μm-sized images (e–h).



bring about a decrease in the Schottky barrier between the metal and the lowest unoccupied molecular orbital (LUMO) of PCBM, in turn associated with an easier electron injection in the PCBM film, paralleled by higher mobility.<sup>45,46</sup> The surface of electrodes from commercial Pd is more hydrophobic (contact angle of  $90.4 \pm 3.5^\circ$ , Fig. S6†) than that of the recycled Pd counterparts ( $85.6 \pm 2.6^\circ$ ).

### Surface morphology

From the AFM images (Fig. 5), we deduce that the root mean square roughness (rms) is  $0.82 \pm 0.13$  nm for the surface of electrodes obtained from commercial Pd and  $0.61 \pm 0.09$  nm for electrodes from recycled Pd. The rms value of the PCBM thin film deposited on commercial Pd electrodes is  $0.54 \pm 0.22$  nm. PCBM films deposited on the recycled Pd electrodes have a smoother surface, with a rms value of  $0.46 \pm 0.03$  nm. The rougher surfaces of commercial Pd electrodes lead to a rougher PCBM thin film, which is expected to induce more structural disorder and defects into the organic thin film, resulting in more charge carrier trapping and lower transport efficiency. This is probably another factor contributing to the better performance of devices based on recycled Pd electrodes compared to commercial Pd ones.

## Conclusions

In conclusion, we demonstrated a sustainable approach for the recovery of Pd, one of the precious metal elements, by utilizing an environmentally benign oxidant, hydrogen peroxide, and a food waste byproduct, lactic acid. Pd was successfully recovered in its metallic state (not cationic, which would require a further reduction step). Recycled Pd (including Ni, after the XPS results) was e-beam evaporated to form the source and drain electrodes of organic field-effect transistors. Surprisingly, recycled Pd-based device performance is better than those of commercial Pd-based ones. Through the investigation of the (surface) chemical composition of the electrodes and structure of thin semiconducting films and electrodes, we explain this result considering the difference in the thickness of the electrodes (higher for recycled Pd electrodes), roughness (lower for recycled Pd electrodes, favourable for a continuous coverage of the electrode surface) and, following the literature, a lower Schottky barrier at the electrode organic semiconducting film interface for Ni-including Pd recycled electrodes.

Work is in progress to (i) extend our approach to other precious metals, like ruthenium and platinum, and (ii) improve the sampling protocols to increase the solidity of the results. Furthermore, we plan to use our recycled Pd electrodes to prepare PdHx protodes to measure proton conductivity in hydrated biomolecular thin films.

## Author contributions

Conceptualization: T. Cecchi and C. Santato; data curation: T. Cecchi, C. Santato, Z. Gao, and Y. Matos Peralta; investigation: T. Cecchi, Z. Gao, O. Girard, C. Clement, and Y. Matos Peralta;

methodology: T. Cecchi, C. Santato, and Z. Gao; funding acquisition: C. Santato; resources: C. Santato and T. Cecchi; supervision: C. Santato and T. Cecchi; writing-original draft: T. Cecchi; writing – review & editing: all authors.

## Conflicts of interest

There are no conflicts to declare.

## Acknowledgements

We thank IIT ‘G. e M. Montani’ for the availability of the infrastructure used for the palladium peeling. We thank GPS Galvanica (Montegiorgio, FM, Italy) and Settimi Galvanica (Macerata Italy) for the donation of the metal wires.

## References

- 1 W. H. Wollaston, *Philos. Trans. R. Soc. London*, 1805, **95**, 316–330.
- 2 H. Chen, N. Brener and J. Callaway, *Phys. Rev. B: Condens. Matter Mater. Phys.*, 1989, **40**, 1443.
- 3 K. S. Song and A. Coskun, *Chimia*, 2023, **77**, 122.
- 4 M. Muscetta, G. Pota, G. Vitiello, S. Al Jitan, G. Palmisano, R. Andreozzi, R. Marotta and I. Di Somma, *React. Chem. Eng.*, 2023, **8**, 661.
- 5 D. J. De Aberasturi, R. Pinedo, I. R. De Larramendi, J. R. De Larramendi and T. Rojo, *Miner. Eng.*, 2011, **24**, 505–513.
- 6 B. Xu, Y. Chen, Y. Zhou, B. Zhang, G. Liu, Q. Li, Y. Yang and T. Jiang, *Metals*, 2022, **12**, 533.
- 7 H. Zheng, Y. Ding, Q. Wen, B. Liu and S. Zhang, *Resour., Conserv. Recycl.*, 2021, **167**, 105417.
- 8 C. J. Rhodes, *Sci. Prog.*, 2019, **102**, 304–350.
- 9 R. G. Charles, P. Douglas, I. L. Hallin, I. Matthews and G. Liversage, *Waste Manage.*, 2017, **60**, 505–520.
- 10 S. Yolcular, *Energy Sources, Part A*, 2016, **38**, 2148–2152.
- 11 J. Emsley, *Nature's Building Blocks: An AZ Guide to the Elements*, Oxford University Press, 2011.
- 12 L. A. Cramer, *JOM*, 2001, **53**, 14–18.
- 13 P. Nuss and M. J. Eckelman, *PLoS One*, 2014, **9**, e101298.
- 14 N. Warner and M. L. Free, *JOM*, 2009, **61**, 27–30.
- 15 B. N. Çetiner, E. U. Yegül, B. Zeytuncu and S. Aktaş, *Desalin. Water Treat.*, 2022, **253**, 211–222.
- 16 A. Nobahar, J. D. Carlier and M. C. Costa, *Clean Technol. Environ. Policy*, 2023, 1–20.
- 17 S. Karim and Y.-P. Ting, *Bioresour. Technol. Rep.*, 2022, **18**, 101069.
- 18 O. Lanaridi, M. Schnürch, A. Limbeck and K. Schröder, *ChemSusChem*, 2022, **15**, e202102262.
- 19 M. C. Costa, A. Assunção, A. M. R. da Costa, C. Nogueira and A. P. Paiva, *Solvent Extr. Ion Exch.*, 2013, **31**, 12–23.
- 20 J. Bauwens, L. S. Rocha and H. M. Soares, *Environ. Sci. Pollut. Res.*, 2022, **29**, 76907–76918.
- 21 R. M. Izatt, S. R. Izatt, N. E. Izatt, K. E. Krakowiak, R. L. Bruening and L. Navarro, *Green Chem.*, 2015, **17**, 2236–2245.



- 22 X. Zhang, Z. Chen, Z. Wan, C. Liu, R. He, X. Xie and Z. Huang, *Int. J. Mol. Sci.*, 2022, **23**, 12158.
- 23 K. S. Song, T. Ashirov, S. N. Talapaneni, A. H. Clark, A. V. Yakimov, M. Nachttegaal, C. Copéret and A. Coskun, *Chem*, 2022, **8**, 2043–2059.
- 24 L. A. Limjucó and F. K. Burnea, *MRS Commun.*, 2022, **12**, 175–182.
- 25 B. Keskin, A. Yuksekdog, B. Zeytuncu and I. Koyuncu, *J. Water Process. Eng.*, 2023, **52**, 103576.
- 26 C. García-Balboa, P. Martínez-Alesón García, V. López-Rodas, E. Costas and B. Baselga-Cervera, *MicrobiologyOpen*, 2022, **11**, e1265.
- 27 T. Cecchi, Z. Gao, C. Clement, A. Camus, A. Karim, O. Girard and C. Santato, *Nanotechnology*, 2022, **34**, 065203.
- 28 Z. Wang, S. Guo and C. Ye, *Procedia Environ. Sci.*, 2016, **31**, 917–924.
- 29 J. J. Bozell and G. R. Petersen, *Green Chem.*, 2010, **12**, 539–554.
- 30 T. Cecchi and C. De Carolis, *Biobased Products from Food Sector Waste*, Springer, 2021.
- 31 G. PALAGHIAS, *Eur. J. Oral Sci.*, 1986, **94**, 267–273.
- 32 J. Talati and A. Patel, *Mater. Corros.*, 1988, **39**, 27–33.
- 33 T. Chen, A. Kitada, K. Fukami and K. Murase, *J. Electrochem. Soc.*, 2019, **166**, D761.
- 34 A. Chumakov, V. Batalova and Y. Slizhov, *AIP Conf. Proc.*, 2016, **1772**, 040004.
- 35 H.-J. Lee, H. Lee and C. Lee, *Chem. Eng. J.*, 2014, **245**, 258–264.
- 36 K. Kim, K. Lee, S. So, S. Cho, M. Lee, K. You, J. Moon and T. Song, *ECS J. Solid State Sci. Technol.*, 2018, **7**, P91.
- 37 N. Wang, T. Zheng, G. Zhang and P. Wang, *J. Environ. Chem. Eng.*, 2016, **4**, 762–787.
- 38 D. G. Castner, K. Hinds and D. W. Grainger, *Langmuir*, 1996, **12**, 5083–5086.
- 39 S. R. Forrest, *Organic Electronics: Foundations to Applications*, Oxford University Press, Oxford, United Kingdom, 2020.
- 40 T. Kanbara, K. Shibata, S. Fujiki, Y. Kubozono, S. Kashino, T. Urisu, M. Sakai, A. Fujiwara, R. Kumashiro and K. Tanigaki, *Chem. Phys. Lett.*, 2003, **379**, 223–229.
- 41 F. Cicoira, C. M. Aguirre and R. Martel, *ACS Nano*, 2011, **5**, 283–290.
- 42 V. D. Mihailetchi, J. K. van Duren, P. W. Blom, J. C. Hummelen, R. A. Janssen, J. M. Kroon, M. T. Rispens, W. J. H. Verhees and M. M. Wienk, *Adv. Funct. Mater.*, 2003, **13**, 43–46.
- 43 J. C. Wataha and K. Shor, *Expert Rev. Med. Devices*, 2010, **7**, 489–501.
- 44 D. R. Lide, *CRC Handbook of Chemistry and Physics*, CRC press, 2004.
- 45 Z. Gao, D. Niyonkuru, A. Yelon and C. Santato, *J. Vac. Sci. Technol., A*, 2023, **41**, 043405.
- 46 E. Wohlfarth, *J. Phys. Chem. Solids*, 1956, **1**, 35–38.

